

Numerical Evaluation of Headed Stud Shear Connector in Composite Beam

Md. Khasro Miah*, Md. Rakibul Hasan and A.K.M. Ruhul Amin

Department of Civil Engineering, Dhaka University of Engineering & Technology, Gazipur, Bangladesh

ABSTRACT

Steel–concrete composite beams are widely used in modern construction due to their structural efficiency, yet the behavior of shear connectors under varying conditions remains insufficiently explored. This study aims to investigate the mechanical performance of composite beams with a focus on the geometry, diameter, and shape of shear connectors. Finite Element Analysis was conducted using ANSYS software, and the numerical model was validated against experimental test data. A parametric study was performed to evaluate the influence of different connector configurations on load-carrying capacity, stiffness, and slip resistance. The results show that increasing the diameter of shear connectors significantly improves both load capacity and stiffness, while square-shaped connectors offer better slip resistance than circular ones. Additionally, stress distribution at mid-span, shear transfer along the beam length, and failure patterns were analyzed. These findings contribute to optimizing shear connector design for improved composite action in steel–concrete systems.

1. INTRODUCTION

Composite structures are widely used in civil engineering construction throughout the world. A composite structure is defined by the interaction of two or more elements acting together as a single element. In a steel-concrete composite beam, the bonding between the steel and the concrete is established by the headed stud shear connector. It creates composite action by resisting the longitudinal sliding and uplifting between the steel beam and concrete slab. This composite structure provides higher strength and stiffness. In the laboratory, specimens test with varying geometric properties is a time-consuming matter, where numerical analysis can easily verify the effect of any variation. In this perspective, a three-dimensional numerical model of a steel-concrete composite beam is prepared by ANSYS software (version 15.0), based on the Finite Elements Method. The model presented here has been investigated by Chapman and Balakrishnan [1] experimentally. The numerical results had been compared with experimental findings. The length of the shear connector with different diameter and shape have also been analyzed as a parametric study. Three-headed stud shear connectors having a length of 76mm, 88mm, and 102mm with a stud shank diameter of $\phi 16\text{mm}$, $\phi 19\text{mm}$, and $\phi 22\text{mm}$ were considered along with the corresponding head diameter of $\phi 25\text{mm}$, $\phi 32\text{mm}$, and $\phi 35\text{mm}$ respectively. Square-headed shear connector has also been introduced to observe the effect of composite action. Based on the analytical result it was found that the effect of length of

stud shear connector is insignificant. On the other hand, increasing the diameter of the shear connector gives higher load caring capacity and stiffness. It is also found that the square shape shear connector gives better stiffness than the circular shear connector. Besides the parametric study, the first cracking load, cracking pattern, normal stress distribution at mid-span, deformation, and shear distribution of the shear connector along the length, have also been observed. Based on the numerical model and its results obtained using finite element software ANSYS well agree with the experimental results.

Several researchers conducted experimental studies on composite beams. Hafez et al. [2] investigated experimentally the performance of simply supported steel-concrete hybrid beams with corrugated webs under vertical loads. The ultimate load of beams with corrugated webs increased by approximately 63% compared to the beam with flat web. Loqman et al. [3] examined bolted shear connectors, which exhibited 95% shear resistance in comparison to headed stud shear connectors. Zhao and Yuan [4] investigated the influence of high-strength engineering materials on overall flexural responses in their experimental examination of steel-concrete composite beams. Full-scale composite beam specimens used to investigate the flexural response with multiple connector options as blind bolt and welded stud [5]. The behaviour of a composite beam with demountable type shear connectors using push-out tests and composite beam testing done by Rehman [6]. Patil and Shaikh [7]

*Corresponding author's email: mkhasro@duet.ac.bd

investigated numerically the effect of shear connections in composite beams using ANSYS software and discovered that the height of the shear connectors had no influence on the composite beam's deflection. The flexural performance

of a hybrid beam with two categories of shear connectors, one being a welded stud and the other being a blind bolt shear connector investigated by Pandilatha and Surumi [8].

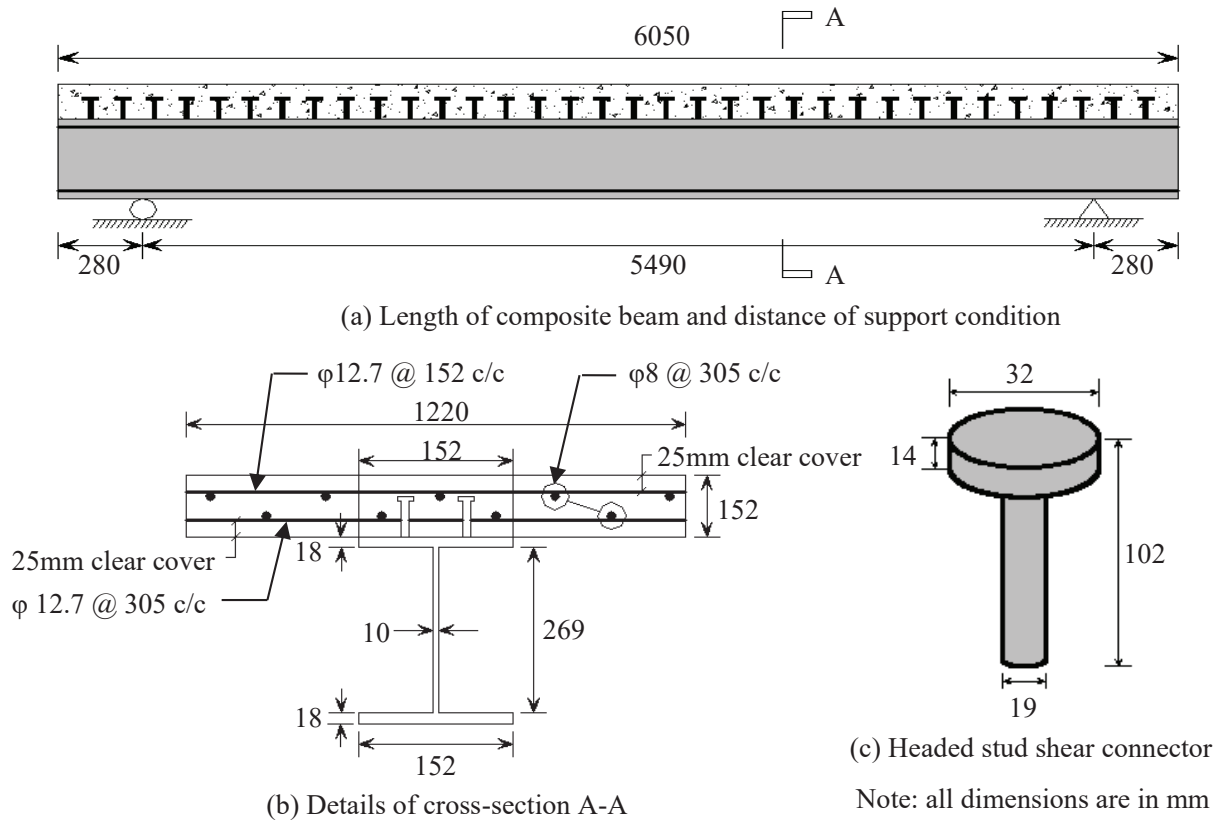


Fig. 1: Geometry of the Composite Beams

Prakash et al. [9] used numerical simulation to evaluate the performance of stud-connected steel-concrete hybrid girders to experimental work and concluded that the FE model is found to predict a conservative value for the ultimate load. Kotinda [10] modeled the structural performance of steel-concrete hybrid simply supported beams numerically by simulating the contact interaction between the surface of the concrete block and the steel joist. Compressive strength of concrete raised from 20MPa to 70MPa enhanced the load bearing capability of a steel-concrete hybrid beam by approximately 20% [11]. Hoffmann *et al.* [12] explores load-slip behavior, shear force distribution along short headed studs, and failure mechanisms including bond and grout degradation in grouted precast joints. Wu *et al.* [13] Focuses on sleeved vs. conventional headed studs using push-out tests and nonlinear Abaqus models. It examines effects of stud height, sleeve geometry, and UHPC filling, reporting a

4–8% capacity increase and 25–35% higher stiffness for sleeved studs.

Even though there have been experiments and computer simulations on shear connectors before, it still doesn't fully understand how different geometrical factors affect the general performance of composite beams. ANSYS, a finite element program, is used to simulate the test results of composite beams in this study, which fills in the gap. After the numerical results matched well with the previous experimental and numerical results of the steel-concrete hybrid or composite beam, a parametric study was also carried out.

2. FINITE ELEMENT MODELING

The numerical simulation used parts from the ANSYS library that had already been defined. The modeling method and choice of elements came from the computer

analysis that Kotinda [10] set up. The next part goes over the different kinds of things that are important for numerical analysis. This study's numerical models matched the actual analysis for model beam "A3" that was done by Chapman and Balakrishnan [1]. Fig. 1 shows the shape of the "A3" beam model.

There are 6050mm of length on the beam and 1220mm of width on the slab. The slab is 152mm thick. The slab is twice as strong because it has 152mm wide flanges on both the top and bottom and steel joists that are 305mm deep. The ring is 18mm thick and the web is 10mm thick. There are two rows of a headed stud shear connection that has a diameter of 19mm. There were 68 shear connections in all. The beam is only held up by a heavy load in the middle of its span.

The concrete slab as shown in Fig. 1 was modeled using SOLID65 element. The element has eight nodes, and each node has three degrees of freedom, which means it can move in x, y, and z directions. A 4-node shell element (SHELL43) is used to represent the steel I-beam. Each node has six degrees of motion. The element can move and rotate around the x, y, and z directions that are attached to it. The three-node beam element BEAM189, which has six degrees of freedom at each node, was used to model the stud shear connection. It can rotate and translate the element along the x, y, and z directions. A two-linear model based on the von Mises criterion that includes isotropic hardening for shear joints. The layer of reinforcement has been added to the SOLID65 element as a real constant. The von Mises criterion says that the best elasto-plastic model for the strengthening steel meets its requirements. The properties of the material and the volume ratio are given as real numbers. Divide the rebar's volume by the total volume of the reinforcement layer to get the volume ratio.

It is easier to connect the slab and steel beam interface with the help of the TARGE170 and CONTA173 elements. When two surfaces touch, pressure is created, but it goes away as soon as the surfaces move apart. This part may also show the friction and cohesion at the point where the concrete slab and steel beam meet, in addition to the pressure characteristics. To keep the number of parts and processing time as low as possible, this study only models the symmetric half of the beam. The load was put on in two stages. At first, the weight of the building was thought to be the gravitational load. In the second step, an outside force is put on the composite beam, focusing it in the middle of its span between two supports.

2.1 Concrete Materials Modeling

The stress-strain curve of concrete, which is shown in Fig. 2, is found using the Mander [14] formulae. Concrete is thought to be a uniform isotropic material. The Mander stress-strain curve for unconfined concrete is shown by Equations (1) and (2).

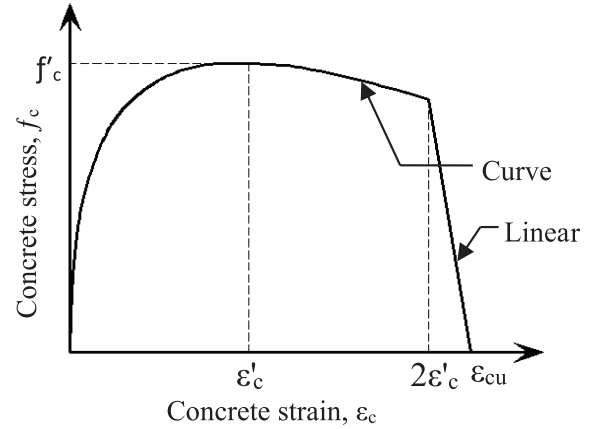


Fig. 2: Mander Stress-strain Curve for Concrete [14]

For $\epsilon_c \leq 2\epsilon'_c$ (curve portion)

$$f_c = \frac{f'_c x r}{r - 1 + x^r} \quad (1)$$

where

$$x = \frac{\epsilon_c}{\epsilon'_c} \text{ and } r = \frac{E_c}{E_c - \left(\frac{f'_c}{\epsilon'_c} \right)}$$

For $2\epsilon'_c < \epsilon_c \leq \epsilon_{cu}$ (linear portion)

$$f_c = \left(\frac{2f'_c r}{r - 1 + 2^r} \right) \left(\frac{\epsilon_{cu} - \epsilon_c}{\epsilon_{cu} - 2\epsilon'_c} \right) \quad (2)$$

where r is as defined previously for the curved portion of the curve. f_c = Concrete stress (MPa), ϵ_c = Concrete strain, E_c = Modulus of elasticity of concrete (MPa), f'_c = Concrete compressive strength (MPa), ϵ'_c = Concrete strain at f'_c , and ϵ_{cu} = Ultimate concrete strain capacity.

2.2 Steel Materials Modeling

The steel yield strain, ϵ_{sy} is determined from $\epsilon_{sy} = f_{sy} / E_s$, where, ϵ_s = Steel strain, f_s = Steel stress (MPa), E_s = Modulus of elasticity of steel (MPa), f_{sy} = Steel yield stress (MPa), f_{su} = Steel maximum stress (MPa), ϵ_{sh} = Strain at onset of strain hardening, ϵ_{su} = Strain corresponding to steel maximum stress, ϵ_r = Strain at steel rupture. The following equations define the simple parametric stress-strain curve for the structural steel as shown in Fig. 3.

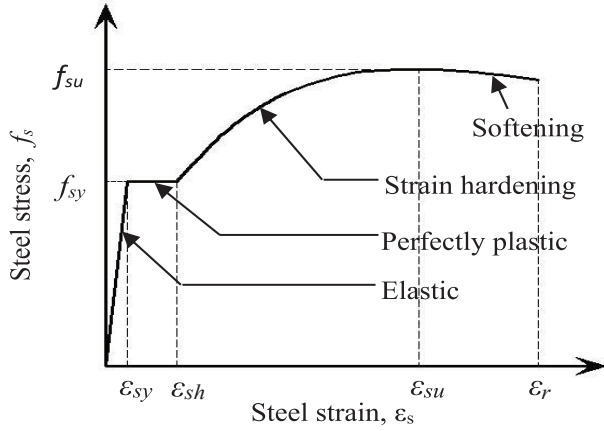


Fig. 3: Structural Steel Parametric Stress-strain Curve [15]

For $\epsilon_s \leq \epsilon_{sy}$ (elastic region),

$$f_s = E_s \epsilon_s$$

For $\epsilon_{sy} < \epsilon_s \leq \epsilon_{sh}$ (perfectly plastic region),

$$f_s = f_{sy}$$

For $\epsilon_{sh} < \epsilon_s \leq \epsilon_r$ (strain hardening and softening regions),

$$f_s = f_{sy} \left[1 + r \left(\frac{f_{su}}{f_{sy}} - 1 \right) e^{(1-r)} \right] \quad (3)$$

where,

$$r = \frac{\epsilon_s - \epsilon_{sh}}{\epsilon_{su} - \epsilon_{sh}}$$

2.3 Finite Element Meshing and Boundary Conditions

In numerical analysis, the mesh size must have fine and consistent in order to have great detail where information is necessary; nevertheless, very fine mesh may require a long time to analyze. In this investigation symmetric half portion of the beam has been considered for modeling because of reducing the elements and computational time. The load was applied in two steps. At the first step, it was considered the weight of the structure itself as the gravitational load. In the second step, applying the external load, concentrated in mid-span between two supports of composite beam as shown in Fig. 4.

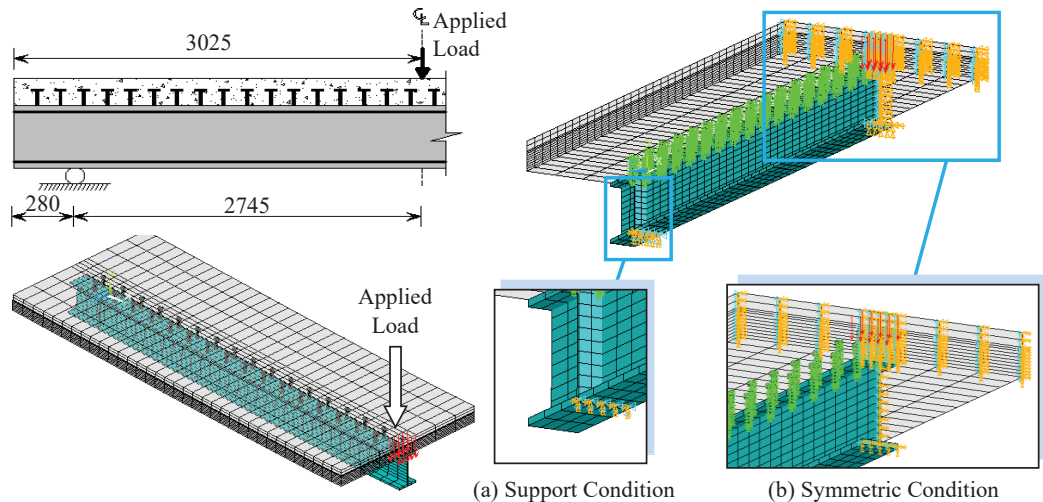


Fig. 4: Symmetric half of the Composite Beam with Single Point Concentrated Load

3. NUMERICAL RESULT

The main thing that was used to check the accuracy of the computer model was the vertical deflection at mid-span under concentrated load. The relative end slip of the composite beam was also looked at.

3.1 Comparison of Numerical Model with Experimental Test Results

Kotinda [10] and Ibrahim et al. [11] conducted numerical analyses on the same model, and their results align closely

with those reported in this study, as illustrated in Fig.5. The experimental applied load and mid span deflection investigated by Chapman and Balakrishnan [1] also shown along with the numerical results in Fig.5. The numerical relationships between load and deflection agree well with both the actual and numerical relationships. The numerical model that was made here is used in the subsequent sections to conduct additional parametric research.

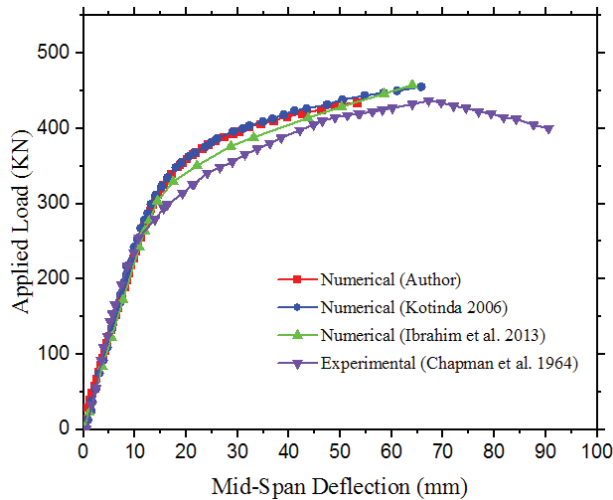


Fig. 5: Load-deflection Curves (Numerical and Experimental)

3.2 Parametric Study

To find out how shear connections affect the performance of composite beams, different shear connector shapes are looked at, and the same model is looked at on its own, as explained in the next parametric study.

3.2.1 Effect of Diameter of Shear Connector

It was looked at how the diameter of the shear connection affects the load-deflection behavior of steel-concrete composite beams by looking at the beams with different diameters of shear connectors. The sizes were $\phi 16\text{mm}$, $\phi 19\text{mm}$, and $\phi 22\text{mm}$, and the stud head widths that went with them were $\phi 25\text{mm}$, $\phi 32\text{mm}$, and $\phi 35\text{mm}$. Table I shows how the diameter of the shear connection affects the behavior of composite beams. The final load capacity goes up by 5.46 percent when the diameter goes from $\phi 16\text{mm}$ to $\phi 22\text{mm}$.

Table I: Ultimate Load Variation Considering Different Diameter of Shear Connectors

Diameter of stud shank (mm)	Connectors Height (mm)	Ultimate Load (kN)	Max. Deflection at Ultimate Load (mm)	Load Capacity Variation (%)
D	H	P_u	Δ_u	$(P_u/P_{D19}) \times 100$
16	102	420.40	44.53	96.66%
19	102	434.90	53.19	100%
22	102	444.12	61.76	102.12%

The findings demonstrate that maximum loading is achieved for connections with a diameter of $\phi 22\text{mm}$, exhibiting reduced vertical deflection. The load-deflection curve for various diameters of the shear connector exhibits nearly identical results across both the linear and non-linear ranges, as illustrated in Fig. 6.

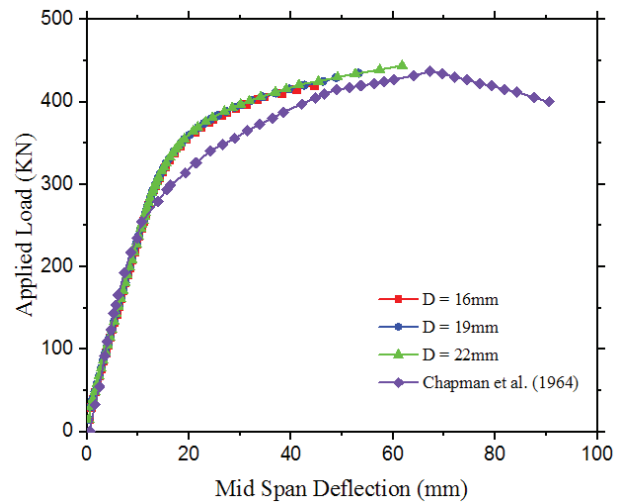


Fig. 6: Load-deflection curves with different diameters of shear connectors

Three different sizes of the shear connection, shown in Table II, were used to test the relative end slip of the composite beam. Increasing the shear connector's diameter makes it much less likely that the concrete block and steel joist will slide along the longitudinal axis. As a result of its lower ultimate load capacity, the $\phi 16\text{mm}$ diameter circular shaped connector shows lower numbers in this study than the $\phi 19\text{mm}$. The slip resistance goes up by 26.17% when the width is raised from $\phi 19\text{mm}$ to $\phi 22\text{mm}$. The load versus slip relation of a composite beam with shear connections of different diameters is shown in Fig. 7.

Table II: End Slip Considering Different Diameter of Shear Connectors

Diameter of stud shank (mm)	Connectors Height (mm)	Ultimate Load (kN)	End Slip at Ultimate Load (mm)	End Slip Variation (%)
D	H	P_u	U_x	$(U_x/U_{D19}) \times 100$
16	102	420.40	0.1334	99.18%
19	102	434.90	0.1345	100%
22	102	444.12	0.0993	73.83%

It is clear from Fig. 7 that as the diameter of a shear connection increases, the relative end slip decreases. In this case, connectors with a diameter of $\phi 22\text{mm}$ do a better job of resisting end slip. Based on our study of how the composite beam behaved, we can say that making the shear connector larger will increase its final load-carrying capacity and make it better at stopping longitudinal sliding.

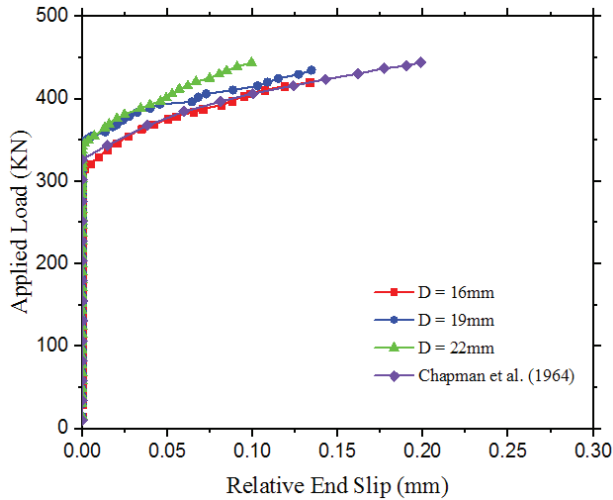


Fig. 7: Load-Slip Curves with Different Diameters of Shear Connectors

3.2.2 Effect of Shape of Shear Connector

The same model was looked at with a square shear connection to see how the shape of the shear connector affected how the load deflected in composite beams. By keeping the same steel area, circular connections with a diameter of $\phi 19\text{mm}$ can be turned into square ones. The body of a square connection is 16.83 mm in size, and the head of that connector is 28.35 mm in size. As shown in Fig. 8, all of the other details about shear connections stay the same.

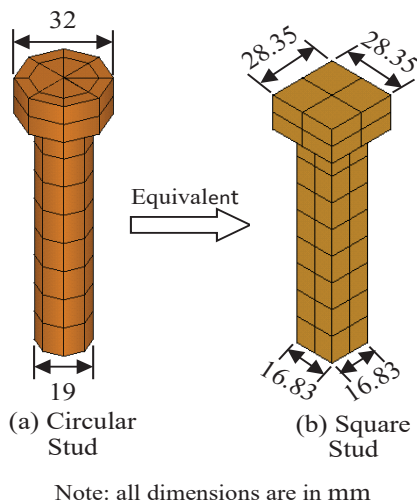


Fig. 8: Dimensions of Circular and Equivalent Square Headed Shear Connector

The data in Table III show that square shear connections can hold a little more weight than circular shear connections. A square connection measuring $16.83\text{mm} \times 16.83\text{mm}$ is the same as a circular connector with a diameter of 19mm , but it can hold 0.92% more weight. As shown in Fig. 9, the load-deflection curve shows that changing the shape of the shear connection doesn't have a big effect on how the composite beam behaves.

Table III: Load Capacity Variation Considering the Different Shape of Shear Connectors

Connectors Shape and size	Connectors Height (mm)	Ultimate Load (kN)	Max. Deflection at Ultimate Load (mm)	Load Capacity Variation (%)
	H	P_u	Δ_u	$(P_u/P_{\text{cir}}) \times 100$
Circular $\phi 19$	102	434.90	53.19	100%
Square 16.83×16.83	102	438.92	58.75	100.92%

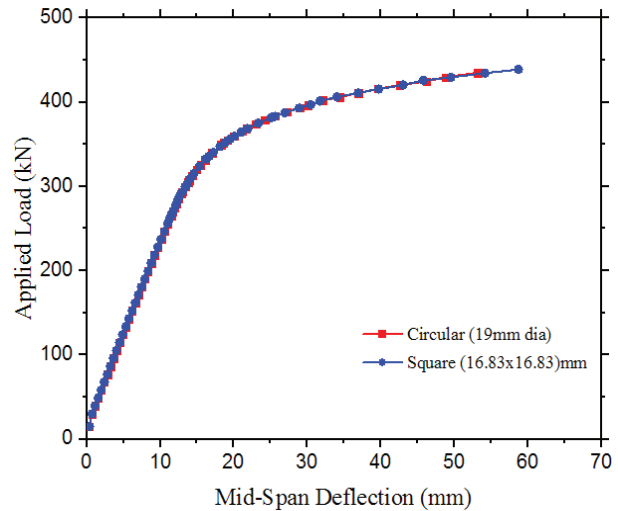


Fig. 9: Load-Deflection Relations with Different Shape of Shear Connectors

The change from a circular to a square shear connection has a small effect on how the load deflects, but the difference in load-relative end slip that happens because of these shape changes is important. Table IV shows that for the $16.83\text{mm} \times 16.83\text{mm}$ square shear connector, the slip drops by 3.50 percent as the ultimate load rises, while

it stays the same for the $\phi 19$ mm circular connector. Fig. 10 shows a load versus slip curve that shows that square connections work slightly better against resistance. This is shown by the end slip in the curve.

3.2.3 Mid Span Stress Distribution along the Depth of Composite Beam Section

Fig. 11 shows how the normal stress is spread along the beam cross-section at the middle of the combined beams (A3). Stress distribution along the ordinate and the concrete slab is under compressive stress above the neutral axis, and the steel joist is under tensile stress below the neutral axis. Because of the composite action, the force distribution in a composite beam is different from that of a normal concrete beam. Fig. 11 shows how the stress is spread out based on the loads.

Table IV: End Slip Variation Considering Different Shape of Shear Connectors

Connectors Shape and size	Connectors Height (mm)	Ultimate Load (kN)	End Slip at Ultimate Load (mm)	End Slip Variation (%)
	H	P_u	U_x	$(U_x/U_{cir}) \times 100$
Circular $\phi 19$	102	434.90	0.1345	100%
Square 16.83×16.83	102	438.92	0.1298	96.50%

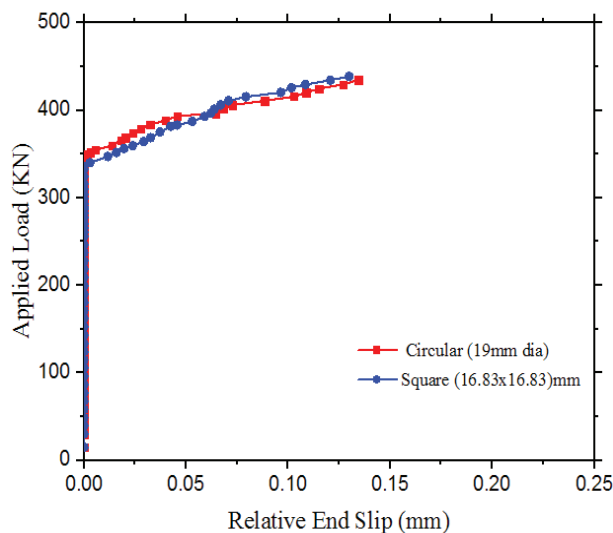


Fig. 10: Load-slip Curve with Different Shape of Shear Connectors

3.2.4 Variation of Shear Force along the Length of Stud Shear Connector

The shear force on the composite system is transferred to the concrete around the shear connection by the bearing forces between them as well. A stud shear connector is put 1458.3 mm from the middle of the span in Fig. 12, which shows how the shear force is transmitted through it. The shear force is zero around the middle of the shear connection shank. Fig. 12 shows that when a certain load of 209.kN is applied, the lower half of the connector's stem resists almost negative shear force, while the upper half resists positive shear force. The connector's head, on the other hand, experiences negative shear and resists vertical separation. In the same way, the shear force distribution along the stud stem follows the same pattern for three different loads viz. 305.02kN, 402.12kN, and 434.90kN with zero shear force at the same location.

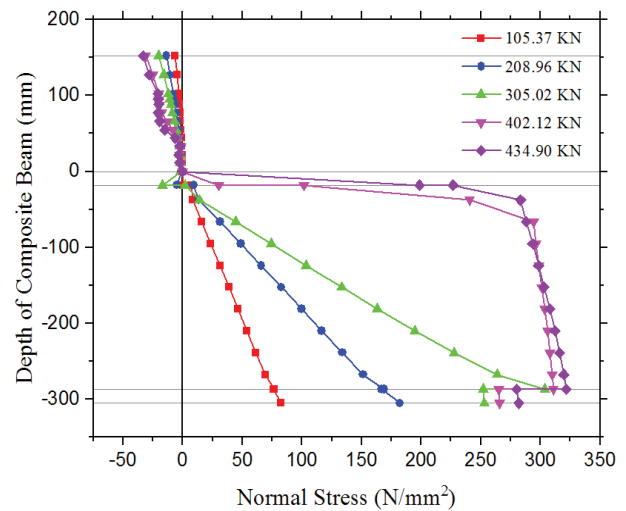


Fig. 11: Mid Span Stress Distribution along the Depth of Composite Beam Section

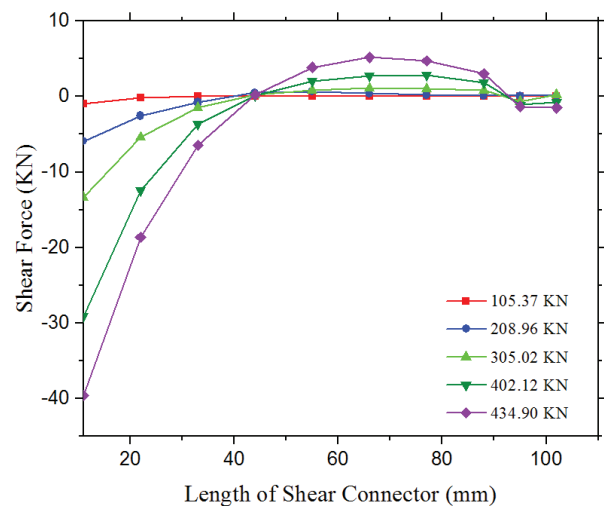


Fig. 12: Shear Force Distribution along the Length of the Shear Connector

3.2.5 Failure of the Composite Beam

According to Chapman and Balakrishnan [1], the failure mode of the composite beam observed in laboratory tests was due to the crushing of the concrete slab at mid-span. In the present numerical analysis, the Von Mises stress distribution shows that the compressive stress at the top surface of the concrete slab exceeds the material's average compressive strength ($f_c = 18.4$ MPa) at a load of 434.90 kN, as illustrated in Fig. 13. This indicates that the concrete reached its ultimate capacity, leading to localized crushing. The stress concentration occurred primarily at mid-span, where maximum compressive forces develop under bending. This corresponds well with the experimental failure pattern. Therefore, the nonlinear finite element model accurately replicates the physical failure mechanism, confirming that the dominant mode of failure in the composite beam is compressive crushing of the concrete slab at mid-span. The convex downward shape in the regions of high stress concentration indicates that compressive stress is dominant in those areas, typically due to load transfer from the slab to the steel beam through the headed studs. In contrast, the concave downward curvature in the low-stress regions represents zones of relatively reduced stress, often due to unloading or redistribution of internal forces.

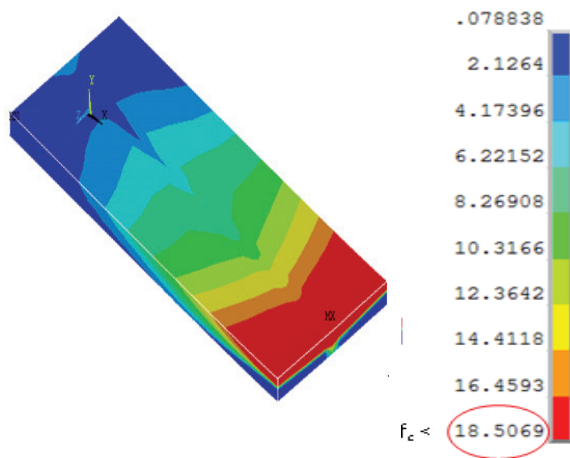


Fig. 13: Von Mess Stress of 434.90 kN

4. CONCLUSIONS

The results of finite element analysis led to the following conclusions:

- The relationship between load and displacement was found to be in good agreement with the numerical results found by Kotinda [10] and Ibrahim et al. [11]. These results showed that

the numerical model that was made was accurate in all respect;

- The numerical model well agreed with experimental results [1] in all respect. The load carrying capacity increase by 5.46% and slip decrease by 26.17% with increasing the stud diameter from 16mm to 22mm.
- When a similar square shear connection (16.83mm x 16.83mm) is used instead of the standard stud shear connector ($\phi 19$ mm), the load-carrying capacity is almost the same, but it is 0.92% higher, and there is 3.50 percent less relative end slip.
- Therefore, a square-shaped shear connector can be used instead of a normal circular shear connector, as long as all the factors are taken into account, such as the ability to hold a load and the resistance to relative end slip.
- Using the model developed here similar research may be performed with different types of shear connectors like; U-type shear connectors, inverted L-type shear connectors, etc. The effect of the variation in concrete strength and steel yield strength on the behaviour of composite beams may also be analysed.

ACKNOWLEDGMENTS

The authors express their profound appreciation to the Department of Civil Engineering, DUET, Gazipur, for their support and collaboration in completing the research effort. This task would not have been accomplished without this unwavering support.

REFERENCES

- [1] J. C. Chapman and S. Balakrishnan, "Experiments on composite beams," *The Structural Engineer*, Vol. 42, pp. 369–383, 1964.
- [2] A. M. A. Hafez, M. M. Ahmed, A. S. Alamar, and A. M. Mahmoud, "Behaviour of simply supported composite concrete-steel beam with corrugated web under vertical loads," *Journal of Engineering Sciences*, Vol. 40, No. 1, 2012.
- [3] N. Loqman, N. A. Safiee, N. A. Bakar, and N. A. M. Nasir, "Structural behaviour of steel-concrete composite beam using bolted shear connectors: A review," *MATEC Web of Conferences*, Vol. 203, 2018.

- [4] H. Zhao and Y. Yuan, "Experimental studies on composite beams with high-strength steel and concrete," *Steel and Composite Structures*, Vol. 10, No. 5, pp. 373–383, 2010.
- [5] W. P. Sameera, B. Uy, O. Mirza, and X. Zhu, "Flexural behavior of composite steel-concrete beams utilizing blind bolt shear connectors," *Engineering Structures*, Vol. 114, pp. 181–194, 2016.
- [6] N. U. Rehman, *Behaviour of Demountable Shear Connectors in Composite Structures*. Bradford, UK: University of Bradford, 2017.
- [7] P. S. Patil and M. G. Shaikh, "A study of effect of shear connector in composite beam in combined bending and shear by ANSYS," *International Journal of Innovative Technology and Exploring Engineering*, No. 3, 2013.
- [8] P. Pandilatha and R. S. Surumi, "Comparative study on flexural behavior of steel concrete composite beam using welded and bolted shear connector," *International Journal of Civil Engineering and Technology*, Vol. 8, No. 5, pp. 1016–1024, May 2017.
- [9] A. Prakash, N. Anandavalli, C. K. Madheswaran, J. Rajasankar, and N. Lakshmanan, "Three-dimensional FE model of stud connected steel-concrete composite girders subjected to monotonic loading," *International Journal of Mechanics and Applications*, Vol. 1, No. 1, 2011.
- [10] T. I. Kotinda, *Numerical Modeling of Steel-Concrete Composite Beams Simply Supported: Emphasis to the Study of the Slab-Beam Interface*. São Carlos, Brazil: University of São Paulo, 2006.
- [11] A. M. Ibrahim and Q. W. Ahmed, "Nonlinear analysis of simply supported composite steel-concrete beam," *Diyala Journal of Engineering Sciences*, Vol. 6, No. 3, pp. 107–126, 2013.
- [12] D. Hoffmann, U. Kuhlmann, J. Schorr, M. Kantar, and J. Völlner, "Composite girders with short headed studs in grouted joints of precast concrete elements—Numerical investigations and design recommendations," *Steel Construction*, Vol. 17, No. 2, pp. 70–80, 2024.
- [13] F. Wu, H. Su, Q. Su, and B. Yuan, "Shear performance study of sleeved stud connectors in continuous composite girder," *Materials*, Vol. 17, No. 13, p. 3326, 2024.
- [14] J. B. Mander, M. J. N. Priestley, and R. Park, "Theoretical stress-strain model for confined concrete," *Journal of Structural Engineering*, Vol. 114, No. 3, pp. 1804–1826, 1988.
- [15] S. Holzer, R. Melosh, and A. E. Somers, *SINDER: A Computer Code for General Analysis of Two-Dimensional Reinforced Concrete Structures*, Report AFWL-TR-74-228, Vol. 1. Kirtland AFB, NM, USA: Air Force Weapons Laboratory, 1975.

